

See discussions, stats, and author profiles for this publication at: <https://www.researchgate.net/publication/6946634>

# Second Hyperpolarizability ( $\gamma$ ) of Singlet Diradical System: Dependence of $\gamma$ on the Diradical Character

ARTICLE in THE JOURNAL OF PHYSICAL CHEMISTRY A · FEBRUARY 2005

Impact Factor: 2.69 · DOI: 10.1021/jp046322x · Source: PubMed

CITATIONS

140

READS

53

10 AUTHORS, INCLUDING:



Masayoshi Nakano

Osaka University

337 PUBLICATIONS 4,769 CITATIONS

SEE PROFILE



Ryohei Kishi

Osaka University

110 PUBLICATIONS 1,947 CITATIONS

SEE PROFILE



Benoît Champagne

University of Namur

401 PUBLICATIONS 8,719 CITATIONS

SEE PROFILE



Edith Botek

Belgian Institute for Space Aeronomy

104 PUBLICATIONS 2,277 CITATIONS

SEE PROFILE

## Second Hyperpolarizability ( $\gamma$ ) of Singlet Diradical System: Dependence of $\gamma$ on the Diradical Character

Masayoshi Nakano,<sup>\*,†</sup> Ryohei Kishi,<sup>†</sup> Tomoshige Nitta,<sup>†</sup> Takashi Kubo,<sup>‡</sup> Kazuhiro Nakasuji,<sup>‡</sup> Kenji Kamada,<sup>§</sup> Koji Ohta,<sup>§</sup> Benoît Champagne,<sup>||</sup> Edith Botek,<sup>||</sup> and Kizashi Yamaguchi<sup>‡</sup>

*Division of Chemical Engineering, Department of Materials Engineering Science, Graduate School of Engineering Science, Osaka University, Toyonaka, Osaka 560-8531, Japan, Department of Chemistry, Graduate School of Science, Osaka University, Toyonaka, Osaka 560-0043, Japan, Photonics Research Institute, National Institute of Advanced Industrial Science and Technology (AIST), Ikeda, Osaka 563-8577, Japan, Laboratoire de Chimie Théorique Appliquée Facultés Universitaires Notre-Dame de la Paix, rue de Bruxelles, 61, 5000 Namur, Belgium*

Received: August 16, 2004; In Final Form: November 5, 2004

The dependence of the second hyperpolarizability ( $\gamma$ ) on the diradical character ( $y$ ) for singlet diradical systems is investigated using a model compound, the *p*-quinodimethane (PQM) molecule with different both-end carbon–carbon (C–C) bond lengths, by several *ab initio* molecular orbital and density functional theory methods. The diradical character based on UHF calculations indicates that at equilibrium geometry PQM is in a singlet ground state and primarily exhibits a quinoid structure, whereas the diradical character increases when increasing both-end C–C bond lengths. At the highest level of approximation, that is, using the UCCSD(T) method with the 6-31G\*+diffuse *p* ( $\zeta = 0.0523$ ) basis set, the longitudinal static  $\gamma$  of PQM presents a maximum value for intermediate diradical character ( $y \approx 0.5$ ) while the  $\gamma$  values are larger for intermediate and large diradical character ( $y \approx 0.5$ – $0.7$ ) than for small diradical character ( $y < 0.2$ ). This feature suggests that the  $\gamma$  values of singlet diradical systems in the intermediate and somewhat strong correlation regimes are significantly enhanced as compared to those in the weak correlation regime. These results are substantiated by a complementary study of the variation in  $\gamma$  upon twisted ethylene.

### 1. Introduction

The nonlinear optical (NLO) properties of molecular systems have been actively studied both theoretically and experimentally over the past 20 years or more<sup>1–10</sup> because organic conjugated compounds exhibit large NLO susceptibilities (hyperpolarizabilities at the microscopic level) with short response times and because of the feasibility of controlling hyperpolarizabilities by the modification of molecular electronic structures. In previous papers,<sup>11–13</sup> we have investigated the variation of the static second hyperpolarizability ( $\gamma$ ) of the H<sub>2</sub> molecule with increasing the bond distance and have found that the  $\gamma$  value first increases, reaches a maximum in the intermediate bond distance region, and then decreases in the bond dissociation region. Moreover, the variation in electronic structure in the dissociation process exemplifies the classification of open-shell systems according to the strength of electron correlation, that is, equilibrium-, intermediate-, and long-bond distance regions correspond to weak-, intermediate-, and strong-correlation regimes, respectively. So, the variation of  $\gamma$  during the dissociation process can be understood by the fact that the intermediate bond breaking nature causes large fluctuations of electrons under the applied electric field. For example, such intermediate bond breaking nature is predicted to be realized

in open-shell neutral radicals with intermediate spin multiplicities, which exhibit significantly enhanced  $\gamma$  values as compared to those in low-spin states using the C<sub>5</sub>H<sub>7</sub> neutral radical model.<sup>14–16</sup> These results indicate the potential of open-shell NLO systems for their application in tunable photonic devices.<sup>7,9,11–25</sup>

On the other hand, such variations in bond breaking nature, that is, variations in the degree of electron correlation, is well described by the diradical character,<sup>26,27</sup> which is an index of the degree of diradical nature and changes from 0 to 1 as a function of the bond dissociation. In fact, several diradical compounds with various diradical characters have been synthesized and different control schemes of the diradical nature have been proposed.<sup>28</sup> Although these compounds are *a priori* interesting in view of their NLO properties, they have not yet been studied. In this study, therefore, we investigate the dependence of  $\gamma$  on the diradical character using singlet diradical model compounds. On the basis of the previous results,<sup>11–16,24</sup> the singlet diradical systems with intermediate and large diradical characters, that is, belonging to the intermediate and strong correlation regimes, are expected to exhibit  $\gamma$  values much larger than that with small diradical characters, that is, belonging to the weak correlation regime. Since the previous studies<sup>12–14,24</sup> show that the electron correlation dependence of  $\gamma$  in the intermediate correlation regime is remarkable, various *ab initio* molecular orbital (MO) and density functional theory (DFT) methods are applied in this study to clarify such dependence for singlet diradical systems with different diradical characters.

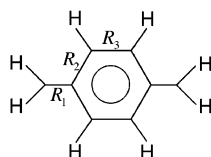
\* Address correspondence to this author.

<sup>†</sup> Department of Materials Engineering Science, Osaka University.

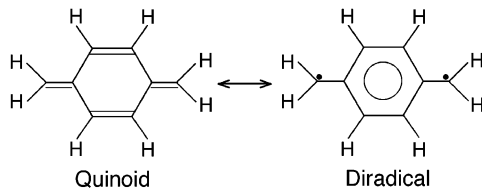
<sup>‡</sup> Department of Chemistry, Osaka University.

<sup>§</sup> National Institute of Advanced Industrial Science and Technology.

<sup>||</sup> Universitaires Notre-Dame de la Paix.

(a) *p*-quinodimethane (PQM) model

(b) Resonance structure

**Figure 1.** Key geometrical parameters of the *p*-quinodimethane molecule (a) and its resonance forms (b).

Finally, the relationships between diradical character and  $\gamma$  values for open-shell neutral systems are discussed in connection with the proposal of a novel class of NLO systems, that is, diradical NLO systems, which also open a path for diradical character-based control of the NLO properties.

## 2. Methodology

**2.1. Model Compounds and Diradical Character.** Figure 1a shows the structure of the *p*-quinodimethane (PQM) molecule in its singlet ground state. It is described by two resonance forms, that is, the quinoid and diradical forms. The quinoid form has no spin sites, whereas the diradical form presents two antiparallel spins at both-end C sites as shown in Figure 1b. In general, the experimental structures of conjugated diradical systems are well reproduced by the RB3LYP and UB3LYP methods.<sup>30</sup> Indeed, the optimized structure for the present system with  $D_{2h}$  symmetry ( $R_1 = 1.351$  Å,  $R_2 = 1.460$  Å, and  $R_3 = 1.346$  Å) at the UB3LYP level (see section 2.2) using 6-311G\* basis set is the same as that at the RB3LYP level (see section 2.2). This result shows that the UB3LYP solution coincides with the RB3LYP solution for the equilibrium geometry. This optimized structure is also in close agreement with the geometrical structure determined at the level of spin-restricted quadratic configuration interaction scheme including all singles and doubles (RQCISD) ( $R_1 = 1.352$  Å,  $R_2 = 1.470$  Å, and  $R_3 = 1.350$  Å), which fairly improves the description of RHF-based solutions in the weak and intermediate correlation regimes.<sup>31</sup> The optimized parameters suggest that PQM presents a large degree of quinoid form instead of diradical nature since  $R_1$  and  $R_3$  are like a C–C double-bond length and are smaller than  $R_2$  having a C–C single-bond nature. To increase the degree of diradical nature, we consider several PQM models with bond length  $R_1$  changing from 1.35 Å to 1.7 Å under the constraint of  $R_2 = R_3 = 1.4$  Å. These boldly approximate models are expected to mimic the change in diradical character of real systems since the variation in  $R_1$  mainly corresponds to the dissociation of  $\pi$  bonds. Although these models lack the concomitant recovery of aromaticity of the central benzene ring present in real systems, our approximate constrained models are considered to be sufficient for the purpose of this study (see Appendix).

To confirm the above speculation, we first determine the diradical character from UHF calculations. The diradical character  $y_i$  related to the HOMO- $i$  and LUMO+ $i$  is defined by the weight of the doubly excited configuration in the MC–

**TABLE 1: Diradical Character  $y$  for  $R_1$ ,  $R_2$ , and  $R_3$  in the PQM Models Shown in Figure 1a<sup>a</sup>**

$R_1$	$R_2$	$R_3$	$y$
1.351	1.460	1.346	0.146
1.350	1.400	1.400	0.257
1.400	1.400	1.400	0.335
1.450	1.400	1.400	0.414
1.500	1.400	1.400	0.491
1.560	1.400	1.400	0.576
1.600	1.400	1.400	0.626
1.700	1.400	1.400	0.731

<sup>a</sup> The first row corresponds to the optimized equilibrium geometry with  $D_{2h}$  symmetry in the singlet ground state.

SCF theory and is formally expressed in the spin-projected UHF (PUHF) theory as<sup>26</sup>

$$y_i = 1 - \frac{2T_i}{1 + T_i^2} \quad (1)$$

where  $T_i$  is the orbital overlap between the corresponding orbital pairs<sup>27</sup> ( $\chi_{\text{HOMO}-i}$  and  $\eta_{\text{HOMO}-i}$ ):

$$\chi_{\text{HOMO}-i} = (\cos \omega)\phi_{\text{HOMO}-i} + (\sin \omega)\phi_{\text{LUMO}+i} \quad (2)$$

and

$$\eta_{\text{HOMO}-i} = (\cos \omega)\phi_{\text{HOMO}-i} - (\sin \omega)\phi_{\text{LUMO}+i} \quad (3)$$

where  $\phi$  and  $\omega$  represent the UHF natural orbital (UNO) and orbital mixing parameter, respectively.  $T_i$  can also be represented by using the occupation numbers ( $n_i$ ) of UNOs:

$$T_i = \frac{\eta_{\text{HOMO}-i} - n_{\text{LUMO}+i}}{2} \quad (4)$$

Since the PUHF diradical characters amount to 0% and 100% for closed-shell and pure diradical states, respectively,  $y_i$  represents the diradical character, that is, the instability of the chemical bond. The present calculation scheme using the UNOs is the simplest but it can well reproduce the diradical characters calculated by other methods such as the ab initio CI method.<sup>30</sup> The present formula employs the UHF NOs instead of UDFT NOs, which leads to incorrect lower diradical character in the present formula. Table 1 gives the diradical characters  $y$  calculated from eqs 1 and 4 using HOMO and LUMO of UNOs for PQM systems with various  $R_1$  values. As expected, the diradical character  $y$  increases when increasing the bond length  $R_1$  starting from the optimized (equilibrium) geometry.

**2.2. Second Hyperpolarizabilities.** We use the 6-31G\*+ $p$  basis set with  $p$  exponent of 0.0523<sup>15,16,29</sup> since several studies have demonstrated that the use of a split-valence or split-valence plus polarization basis set augmented with a set of  $p$  and/or  $d$  diffuse functions on the second-row atoms enables us to reproduce the second hyperpolarizabilities of large- and medium-size  $\pi$ -conjugated systems calculated with larger basis sets.<sup>14,29,32</sup> The spin-restricted (R) and spin-unrestricted (U) type Hartree–Fock (HF) and post-HF methods are employed. The post-R(U)HF methods include the R(U)HF–Møller–Plesset  $n$ th-order perturbation (R(U)MP $n$  ( $n = 2-4$ )), the R(U)HF-coupled-cluster with single and double excitations (R(U)CCSD) as well as with a perturbative treatment of the triple excitations, (R(U)CCSD(T)). The RHF-based post-HF methods break down in the dissociation (strong correlation) regime since the starting RHF solution is heavily triplet-unstable.<sup>31,33-38</sup> Even higher-order excitation operators, such as SD(T) in RCC treatment,<sup>31</sup>

**TABLE 2:**  $\gamma$  [ $\times 10^2$  au] for PQM Models with Different Diradical Characters  $y$  at the RHF, UHF, RMP2, UMP2, APUMP2, UCCSD(T), and UBHandHLYP Levels

Y	RHF	UHF	RMP2	UMP2	APUMP2	UCCSD(T)	UBHandHLYP
0.146	-7.709	260.8	273.0	765.4	433.1	232.7	546.9
0.257	-78.84	218.5	477.0	630.5	468.4	459.6	641.1
0.335	-143.2	204.0	774.8	596.9	559.9	628.4	678.0
0.414	-243.0	184.8	1305	544.7	606.9	749.0	688.1
0.491	-393.6	164.6	2249	478.5	575.5	775.4	671.6
0.576	-671.9	141.7	4428	410.1	515.7	737.2	620.6
0.626	-941.3	127.4	7040	363.3	427.5	680.6	572.5
0.731	-2103	99.28	23250	255.1	132.2	488.1	433.7

are not necessarily adequate for removing the deficient behavior for many electron systems. On the other hand, the UHF and UMP $n$  methods significantly suffer from spin contamination effects and give a small hump in the intermediate bond-dissociation region of the potential energy curve<sup>31</sup> and exhibit incorrect variation in  $\gamma$  in the dissociation process of diatomic molecules.<sup>12,13</sup> Therefore, the approximate spin-projected UHF and UMP2, that is, APUHF and APUMP2,<sup>31</sup> have also been applied to highlight the effects of spin contamination corrections on  $\gamma$ . In this scheme, the lowest spin (LS) UHF-based solutions are projected only by the corresponding highest spin (HS) solutions. The APUHF X energy is given by<sup>31</sup>

$${}^{\text{LS}}E_{\text{APUHF}} = {}^{\text{LS}}E_{\text{UHF}} + f_{\text{SC}}[{}^{\text{LS}}E_{\text{UHF}} - {}^{\text{HS}}E_{\text{UHF}}] \quad (5)$$

where  ${}^{\text{Y}}E_{\text{UHF}}$  denotes the total energy of the spin state Y determined at the X post-HF level on the basis of the UHF solution. The factor  $f_{\text{SC}}$  for a spin multiplet ( $2s + 1$ ) is the fraction of spin contamination given by

$$f_{\text{SC}} = \frac{{}^{\text{LS}}\langle S^2 \rangle_{\text{UHF}} - s(s+1)}{{}^{\text{HS}}\langle S^2 \rangle_{\text{UHF}} - {}^{\text{LS}}\langle S^2 \rangle_{\text{UHF}}} \quad (6)$$

The AP UHF X methods (X = MP $n$ , CC, etc.) have been successfully applied to the calculations of potential energy surfaces,<sup>31</sup> effective exchange integrals in the Heisenberg models for open-shell clusters,<sup>26,31,33–35</sup> and hyperpolarizabilities of H<sub>2</sub> in the bond-breaking region.<sup>12,13</sup> Among the density functional theory (DFT) schemes, the spin-restricted (R) and unrestricted (U) hybrid B3LYP and BHandHLYP exchange-correlation functionals have been adopted. All calculations have been performed using the Gaussian 98 program package.<sup>39</sup>

We confine our attention to the dominant longitudinal component of static  $\gamma$ , which is considered to be a good approximation to off-resonant dynamic  $\gamma$ . The static  $\gamma$  can be obtained by the finite field (FF) approach<sup>40</sup> which consists in the fourth-order differentiation of energy  $E$  with respect to different amplitudes of the applied external electric field. We adopt a four-point procedure (equivalent to a seven-point procedure for a nonsymmetric case) using field amplitudes of 0.0, 0.0010, 0.0020, and 0.0030 au:<sup>25</sup>

$$\gamma = \{E(3F) - 12E(2F) + 39E(F) - 56E(0) + 39E(-F) - 12E(-2F) + (-3F)\}/36(F)^4 \quad (7)$$

Here,  $E(F)$  indicates the total energy in the presence of the field  $F$  applied in the longitudinal direction. This has enabled us to reach an accuracy of 10–100 au on the static longitudinal  $\gamma$ .

### 3. Results and Discussion

Table 2 provides the  $\gamma$  values for PQM models with different diradical characters at the RHF, UHF, RMP2, UMP2, APUMP2, UCCSD(T), and UBHandHLYP levels. The  $\gamma$  values are given

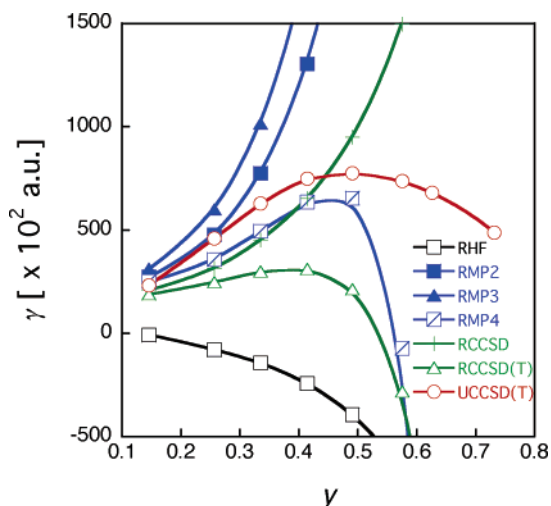


**Figure 2.** Diradical character ( $y$ ) dependence of  $\gamma$  [au] for the PQM models. The RHF, RMP2, RMP3, RMP4, RCCSD, and RCCSD(T) results as well as the UCCSD(T) results using 6-31G\*+ $p$  ( $\zeta = 0.0523$ ) basis sets are shown.

in atomic units (au), which can be converted to other units by the relation  $1 \text{ au} = 5.0366 \times 10^{-40} \text{ esu} = 6.2353 \times 10^{-65} \text{ Cm}^4/\text{V}^3$ .

Figure 2 shows the results calculated by the spin-restricted (R) HF based methods as well as the UCCSD(T) result. Among the different levels of approximation, the UCCSD(T) method is considered to provide the most reliable results for the present systems. As expected, it turns out that the  $\gamma$  value at the UCCSD(T) level increases with increasing  $y$  in the weak diradical region ( $y = 0.1$ – $0.5$ ), attains a maximum in the intermediate region ( $y \approx 0.5$ ), and then decreases in the region corresponding to large diradical character ( $y > 0.5$ ). The maximum  $\gamma$  value at the UCCSD(T) level (77500 au) for a  $y$  value close to 0.5 is 3.3 times as large as the value at the equilibrium geometry (23300 au) ( $y = 0.146$ ). The RHF  $\gamma$  value is negative while its magnitude increases strongly with the diradical character. The inclusion of electron correlation at the RMP $n$  ( $n = 2$ – $4$ ) levels cannot correct this deficient behavior: at the RMP2 and RMP3 levels  $\gamma$  is positive but displays a sharp and overshoot increase with  $y$ , while at the RMP4 level the evolution as a function of  $y$  is correctly reproduced up to  $y = 0.4$  but deviates toward too negative values for larger  $y$  values. Even the RCC methods cannot correct such wrong behavior though the RCCSD and RCCSD(T) methods rather suppress the overshooting behavior of the RMP $n$  results ( $n = 2, 3$ ). Such incorrect behavior is predicted to originate from the triplet instability of the RHF solution in the intermediate and strong correlation regimes.<sup>31,35–37</sup>

Figure 3 shows the results obtained by the UHF-based methods. Although for the equilibrium geometry the UHF method nicely reproduces the UCCSD(T)  $\gamma$  value, the UMP $n$  ( $n = 2$ – $4$ ) methods overshoot  $\gamma$ . At the UHF and UMP $n$  levels,



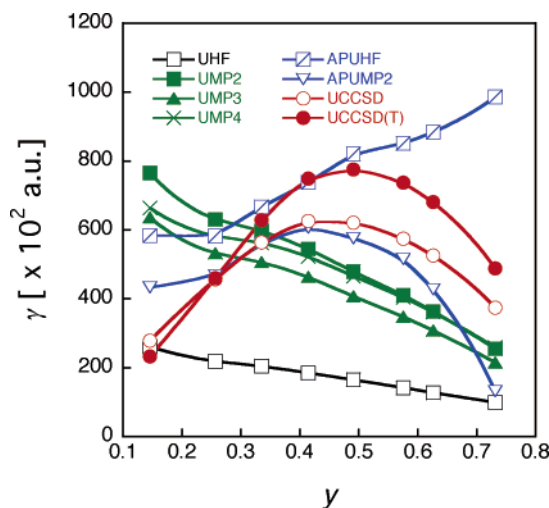


**Figure 3.** Diradical character ( $y$ ) dependence of  $\gamma$  [au] for the PQM models. The UHF, UMP2, UMP3, UMP4, APUHF, APUMP2, UCCSD, and UCCSD(T) results using 6-31G\*+ $p$  basis sets are shown.

$\gamma$  monotonically decreases with increasing diradical character, so that for  $y$  smaller than 0.3 they are larger than the UCCSD(T) reference value, whereas they are smaller in the intermediate and large diradical character regions. Adopting the APUHF method, the behavior of  $\gamma$  for  $y$  is different:  $\gamma$  increases with increasing diradical character. In contrast, the  $\gamma$  values determined at the APUMP2 level are significantly improved as compared to those at the UHF, UMP $n$ , and APUHF levels and qualitatively reproduce the results obtained at the UCCSD level. To obtain a better agreement with the UCCSD(T) results, higher-order correlation methods, that is, APUMP3 and APUMP4 methods, are predicted to be required. This suggests that not only the nondynamical correlation involved at the APUHF level but also the dynamical correlation involved at the APUMP $n$  levels are indispensable for the description of  $\gamma$  of open-shell singlet systems. Similarly to the neutral doublet  $C_3H_7$  radical system,<sup>14</sup> obtaining a fast convergence of  $\gamma$  for open-shell singlet systems with respect to the order of electron correlation requires first the removal of spin contamination. The UCCSD method turns out to reproduce qualitatively the variations in  $\gamma$  obtained at the UCCSD(T) level, whereas the triple excitations become important for a quantitative description in the regions with intermediate and large diradical characters ( $y > 0.25$ ).

Figure 4 displays the diradical character dependences of  $\gamma$  evaluated by DFT methods as well as the UCCSD(T) scheme for comparison. The RB3LYP and RBHandHLYP methods undershoot the UCCSD(T)  $\gamma$  value. In addition, although for equilibrium geometry they provide similar  $\gamma$  values, the RB3LYP value increases with  $y$ , whereas it decreases using the RBHandHLYP exchange-correlation functional. The UB3LYP results give the same results as the RB3LYP results until  $y \approx 0.25$ , while an abrupt increase is observed around  $y = 0.3$ . After the abrupt increase,  $\gamma$  overshoots the UCCSD(T) value and then increases steadily. In contrast, the UBHandHLYP method provides a similar qualitative description of the variation in  $\gamma$  to that at the UCCSD(T) level. Nevertheless, the  $\gamma$  values at the UBHandHLYP level overshoot that at the UCCSD(T) level in the region with small diradical character ( $y < 0.3$ ), while the  $\gamma$  values at the UBHandHLYP level are slightly smaller than those at the UCCSD(T) level in the region with intermediate and large diradical characters ( $y > 0.4$ ). Moreover, the value of  $y$  corresponding to the maximum of  $\gamma$  is slightly different at the UBHandHLYP and UCCSD(T) levels of approximation.

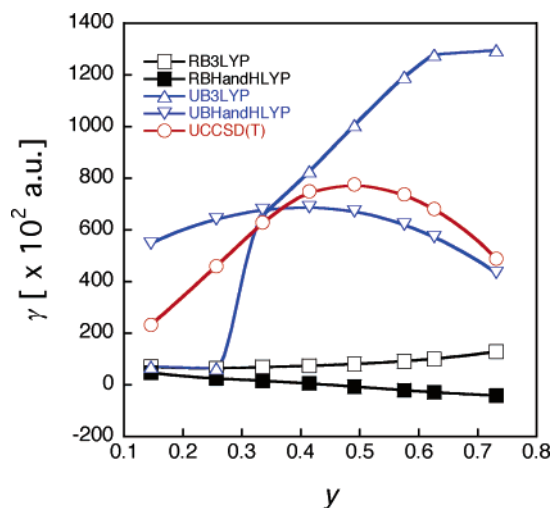


**Figure 4.** Diradical character ( $y$ ) dependence of  $\gamma$  [au] for the PQM models. The RB3LYP, RBHandHLYP, UB3LYP, and UBHandHLYP results as well as the UCCSD(T) results using 6-31G\*+ $p$  basis sets are shown.

Judging from the present results, it is predicted that hybrid DFT methods with exchange-correlation functionals specifically tuned for reproducing the NLO properties of diradical species could provide satisfactory results in comparison with the more elaborated UCCSD(T) scheme. However, it remains to be assessed whether a given tuned functional can perform efficiently for a large range of diradicals.

The variation in  $\gamma$  for the PQM models with increasing diradical character can be understood from the analogy with the dissociation of  $H_2$ . The increase of  $\gamma$  in the intermediate diradical character region is predicted to be caused by the virtual excitation processes with zwitterionic contribution between the radicals on both-end carbon atoms, which corresponds to the intermediate dissociation region for the  $H_2$  molecule.<sup>11</sup> In an analogical way, the intermediately spatial polarized wave functions for  $\alpha$  and  $\beta$  radical spins on both-end carbon sites in the PQM with intermediate radical character are predicted to contribute to the enhancement of  $\gamma$  through the virtual excitation processes involving the zwitterionic nature as compared to the small diradical character region with a stable bond nature, giving a relatively small polarization. On the other hand, in the large radical character (strong correlation or magnetic) region, the localized spins on both-end sites exhibit less charge polarization to the applied external electric field because of its strong correlation nature, so that the  $\gamma$  value decreases again.

Although the present results on the diradical character dependence of  $\gamma$  for PQM models are predicted to be valid for other aromatic singlet diradical systems, it is worth examining the applicability of the present result to nonaromatic singlet diradical systems using models except for the  $H_2$  dissociation model.<sup>11</sup> The twisted ethylene models (with twisted angle  $\theta$ ) are considered to be suitable for exhibiting the increase in diradical character ( $y$ ) by increasing the twisted angle. In fact, the highly electron-correlated ab initio MO results for longitudinal  $\gamma$  of twisted ethylene models up to  $\theta = 75^\circ$  ( $y \sim 0.5$ ) have predicted the increase in  $\gamma$  with increasing the twisted angle, that is, diradical character.<sup>24</sup> To clarify the variation in  $\gamma$  for  $y$  larger than 0.5, we consider the ethylene models with  $\theta$  changing from  $55^\circ$  to  $90^\circ$  as shown in Figure 5a. The C–C bond length (1.3376 Å), C–H bond length (1.0868 Å), and H–C–H bond angle ( $121.58^\circ$ ), which are optimized using the QCISD method with 6-311G\*\* basis set for the equilibrium planar ethylene, are used for all twisted ethylene models. As

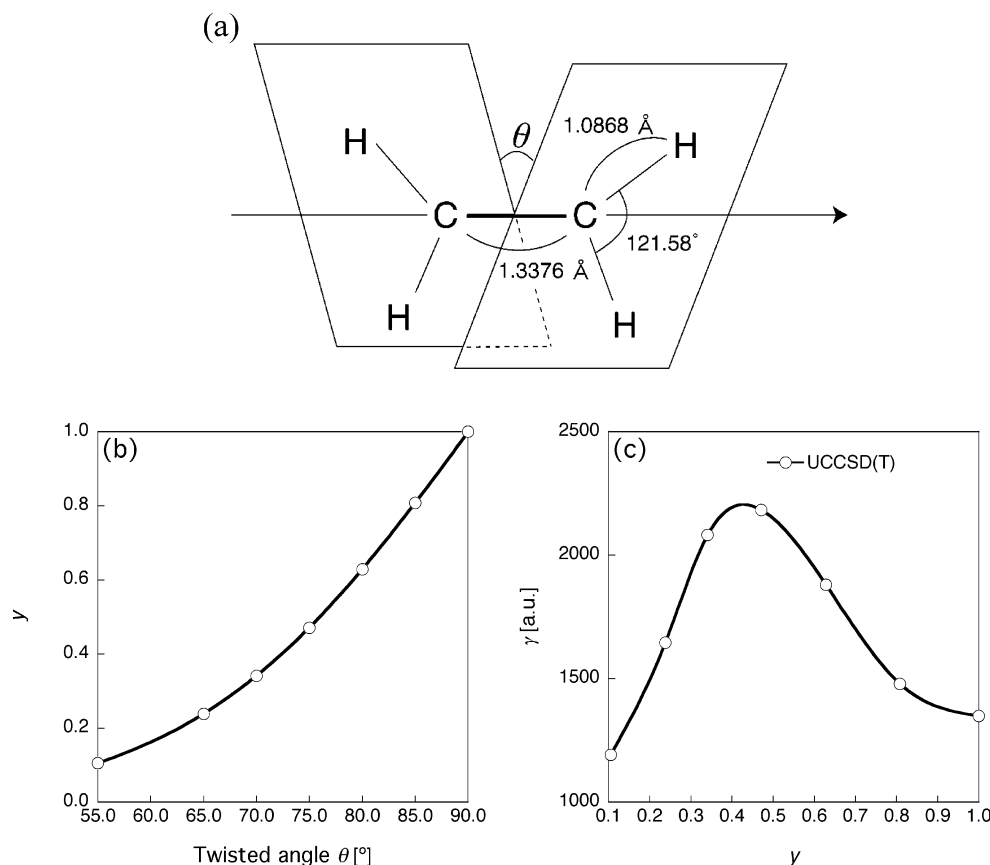


**Figure 5.** Twisted ethylene model (a), diradical character ( $\gamma$ ) versus twisted angle  $\theta$  [°] (b), and longitudinal  $\gamma$  value [a.u.] versus  $\gamma$ . The C–C and C–H bond distances and H–C–H bond angle used for twisted ethylene models are optimized at the UQCISD/6-311G\*\* level for the planar equilibrium geometry. The  $\gamma$  values are calculated by the UCCSD(T) method with 6-31G\*\*+*sp* basis set.

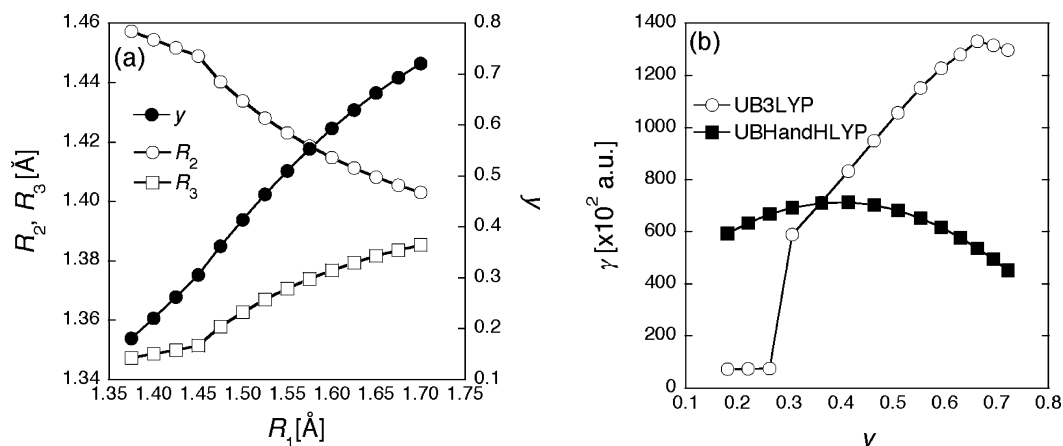


**Figure 6.** Variation in diradical character ( $\gamma$ ) and bond lengths ( $R_2$  and  $R_3$ ) with increasing  $R_1$  (a) and the  $\gamma$  values versus  $\gamma$  at the UB3LYP and UBHandHLYP levels with 6-31G\*\*+*p* basis set (b).  $R_2$  and  $R_3$  are optimized using the UB3LYP/6-311G\* method for each  $R_1$ .

shown in Figure 5b, the diradical character  $\gamma$  using the occupation numbers of UNOs varies from 0.1 to 1.0 with increasing the twisted angle changing from 55° to 90°. The diradical character dependence of  $\gamma$  values at the UCCSD(T) level with 6-31G\*\*+*sp* basis set ( $\zeta = 0.0523$  on C atoms and  $\zeta_{s,p} = 0.0406$  on H atoms) is shown in Figure 5c. Similarly to the results for PQM models, the  $\gamma$  values increase with increasing  $\gamma$  ( $<0.5$ ), attain the maximum value around  $\gamma \sim 0.5$ , and then decrease in the region  $\gamma > 0.5$ . The maximum  $\gamma$  value (2184 au) at  $\gamma \sim 0.5$  is about 4.1 times as large as that (536 au) at  $\gamma = 0$  (equilibrium planar structure). Judging from these two results (PQM and twisted ethylene models) and the previous results for H<sub>2</sub> dissociation model, the diradical character dependence of  $\gamma$  obtained in this study is expected to be applied

to general singlet diradical systems including aromatic and nonaromatic systems though further investigation of other singlet diradical systems, for example, heteroatomic systems, are necessary for confirming the applicability of the present structure–property relation in  $\gamma$ .

#### 4. Concluding Remarks

The dependence of the second hyperpolarizability ( $\gamma$ ) on the diradical character is investigated for *p*-quinodimethane (PQM) models by changing both-end C–C bond lengths. It turns out that, using the reference UCCSD(T) results,  $\gamma$  increases with the diradical character ( $\gamma$ ) in the region where  $\gamma < 0.5$ , attains a maximum in the region with intermediate diradical character

( $\gamma \approx 0.5$ ), and then decreases. The inclusion of high-order electron correlation effects is indispensable for reproducing the qualitative variations in  $\gamma$  as a function of the diradical character. Indeed, the APUMP2 and UCCSD methods qualitatively provide the same variations of  $\gamma$  as the UCCSD(T) scheme. This feature suggests that the (approximate) spin projection schemes with relatively low-order electron correlations, for example, APUMPn, effectively include both nondynamical and dynamical correlations in a well-balanced manner for neutral open-shell singlet systems in the intermediate correlation region, not only in the ground state but also in the excited states. Judging from the similarity of the variation in  $\gamma$  ( $\gamma > 0.4$ ) between the UBHandHLYP and UCCSD(T) results, the DFT methods with tuned hybrid exchange-correlation functionals can reproduce the  $\gamma$  values of singlet diradical systems for a broad range of diradical characters, in an analogy to the case of tuning parameters in the hybrid exchange-correlation functional to reproduce the effective exchange integral for open-shell systems at the UCCSD(T) level.<sup>40,41</sup> Furthermore, several recently developed approaches based on the spin-flip (SF) model,<sup>43</sup> for example, SF-CI, SF-EOM, and SF-TDDFT, for bond-breaking processes and singlet diradical systems are expected to be interesting schemes for further investigation of the hyperpolarizabilities of singlet diradical systems.

On the basis of the same dependence of  $\gamma$  on the diradical character observed for H<sub>2</sub> dissociation model,<sup>11</sup> *p*-quinodimethane model, and twisted ethylene model, we can conclude that the  $\gamma$  values of singlet diradical systems presenting the intermediate or somewhat large diradical characters tend to be significantly enhanced as compared to those of conventional NLO materials small or zero diradical characters. The variation in  $\gamma$  with the diradical character also suggests the possibility of using singlet diradical compounds as novel NLO systems, which could be tuned to match the desired properties, since several singlet diradical systems with controlled diradical characters can actually be synthesized.<sup>28</sup> The investigation of the NLO properties of practical diradical systems is now in progress in our laboratory.

**Acknowledgment.** This work was supported by Grant-in-Aid for Scientific Research (B) (No. 14340184) from Japan Society for the Promotion of Science (JSPS). E. B. thanks the Interuniversity Attraction Pole on "Supramolecular Chemistry and Supramolecular Catalysis" (IUAP N° P5-03) for her postdoctoral grant. B. C. thanks the Belgian National Fund for Scientific Research for his Senior Research Associate position.

## Appendix

In this study, we employ a constrained model, in which  $R_1$  varies, while  $R_2$  and  $R_3$  are fixed to 1.4 Å though the increase in  $R_1$  should affect the values of  $R_2$  and  $R_3$  through the recovery of the aromaticity of the central benzene ring. To confirm the validity of our constrained model, we examine a relaxed model by performing optimization (with a constraint of  $D_{2h}$  symmetry) of geometries except for  $R_1$ . As shown in Figure 6a, the increase in  $R_1$  causes a monotonic increase in diradical character  $\gamma$  as well as the increase in  $R_3$  and the decrease in  $R_2$ . Namely,  $R_2$  and  $R_3$  approach 1.4 Å in the limit of large  $R_1$ . This feature is in agreement with the speculation on the basis of the two resonance forms, that is, the quinoid and diradical forms, mentioned above. The UBHandHLYP and UB3LYP results using this relaxed model shown in Figure 6b display the same  $\gamma$ -dependence as with the constrained model ( $R_2 = R_3 = 1.4$

Å) (see Figure 4). Therefore, our constrained model appears to be satisfactory for the purpose of the present study.

## References and Notes

- (1) *Nonlinear Optical Properties of Organic and Polymeric Materials*; Williams, D. J., Ed.; ACS Symposium Series 233; American Chemical Society: Washington, DC, 1984.
- (2) *Nonlinear optical properties of organic molecules and crystals*; Chemla, D. S., Zyss, J., Eds.; Academic Press: New York, 1987; Vols. 1–2.
- (3) Prasad, N. P.; Williams, D. J. *Introduction to Nonlinear Optical Effects in Molecules and Polymers*; Wiley: New York, 1991.
- (4) *Optical Nonlinearities in Chemistry Chem. Rev.*; Michl, J., Ed.; 1994; Vol. 94, American Chemical Society: Washington, DC.
- (5) *Nonlinear Optical Materials. Theory and Modeling*; Karna, S. P., Yeates, A. T., Eds.; ACS Symposium Series 628; American Chemical Society: Washington, DC, 1996.
- (6) Bosshard, Ch.; Sutter, K.; Prêtre, Ph.; Hulliger, J.; Flosheimer, M.; Kaatz, P.; Günter, P. *Organic Nonlinear Optical Materials*; Gordon and Breach: New York, 1995.
- (7) Nakano, M.; Yamaguchi, K. In *Trends in Chemical Physics*; Research trends; Brown, R. D., Ed., Trivandrum, India, 1997; Vol. 5, pp 87–237.
- (8) *Handbook of Advanced Electronic and Photonic Materials and Devices, Nonlinear Optical Materials*; Nalwa, H. S., Ed.; Academic Press: New York, 2001; Vol. 9.
- (9) Nakano, M.; Yamaguchi, K. Mechanism of Nonlinear Optical Phenomena for  $\pi$ -Conjugated Systems. In *Organometallic Conjugation*; Nakamura, A., Ueyama, N., Yamaguchi, K., Eds.; Kodansha and Springer: Tokyo, 2002.
- (10) Nakano, M.; Yamaguchi, K. In *Advances in Multi-Photon Processes and Spectroscopy*; Lin, S. H., Villayes, A. A., Fujimura, Y., Eds., World Scientific: Singapore, 2003; Vol. 15, pp 1–146.
- (11) Nakano, M.; Nagao, H.; Yamaguchi, K. *Phys. Rev. A* **1997**, *55*, 1503.
- (12) Nakano, M.; Yamada, S.; Kishi, R.; Takahata, M.; Nitta, T.; Yamaguchi, K. *J. Nonlinear Opt. Phys. Mater.* in press.
- (13) Nakano, M.; Yamada, S.; Yamaguchi, K. *J. Comput. Meth. Science Eng.*, in press.
- (14) Nakano, M.; Nitta, T.; Yamaguchi, K.; Champagne, B.; Botek, E. *J. Phys. Chem. A* **2004**, *108*, 4105.
- (15) Nakano, M.; Champagne, B.; Botek, E.; Kishi, R.; Nitta, T.; Yamaguchi, K., *Proceedings of CIMTEC*, in press.
- (16) Nakano, M.; Champagne, B.; Botek, E.; Kishi, R.; Nitta, T.; Yamaguchi, K., *Synth. Met.* submitted.
- (17) Nakano, M.; Yamaguchi, K. *Chem. Phys. Lett.* **1993**, *206*, 285.
- (18) Di Bella, S.; Fragalà, I.; Ledoux, I.; Marks, T. J. *J. Am. Chem. Soc.* **1995**, *117*, 9481.
- (19) Karna, S. P. *J. Chem. Phys.* **1996**, *104*, 6590; **1996**, *105*, 6091.
- (20) Nakano, M.; Yamada, S.; Yamaguchi, K. *Bull. Chem. Soc. Jpn.* **1998**, *71*, 845.
- (21) Yamada, S.; Nakano, M.; Yamaguchi, K. *J. Phys. Chem. A* **1999**, *103*, 7105.
- (22) Nakano, M.; Yamada, S.; Yamaguchi, K. *Chem. Phys. Lett.* **1999**, *311*, 221.
- (23) Champagne, B.; Kirtman, B. *Chem. Phys.* **1999**, *245*, 213.
- (24) Yamada, S.; Nakano, M.; Yamaguchi, K. *Int. J. Quantum Chem.* **1999**, *71*, 177.
- (25) Nakano, M.; Shigemoto, I.; Yamada, S.; Yamaguchi, K. *J. Chem. Phys.* **1995**, *103*, 4175.
- (26) Yamaguchi, K. *Self-Consistent Field Theory and Applications*; Carbo, R., Klobukowski, M., Eds.; Elsevier: Amsterdam, 1990, p 727.
- (27) Yamaguchi, K.; Okumura, M.; Takada, K.; Yamanaka, S. *Int. J. Quantum Chem. Symp.* **1993**, *27*, 501.
- (28) (a) Scheschkewitz, D.; Amii, H.; Gomitza, H.; Schoeller, W. W.; Bourissou, D.; Bertrand, G. *Angew. Chem., Int. Ed.* **2004**, *43*, 585. (b) Scheschkewitz, D.; Amii, H.; Gomitza, H.; Schoeller, W. W.; Bourissou, D.; Bertrand, G. *Science* **2002**, *295*, 1880. (c) McMasters, D. R.; Wirz, J. *J. Am. Chem. Soc.* **2001**, *123*, 238. (d) Sugiyama, H.; Ito, S.; Yoshifuji, M. *Angew. Chem., Int. Ed.* **2003**, *42*, 3802. (e) Niecke, E.; Fuchs, A.; Baumeister, F.; Nieger, M.; Schoeller, W. W. *Angew. Chem., Int. Ed. Engl.* **1995**, *34*, 555.
- (29) Hurst, G. J. B.; Dupuis, M.; Clementi, E. *J. Chem. Phys.* **1988**, *89*, 385.
- (30) (a) Herebian, D.; Wiegardt, K. E.; Neese F. *J. Am. Chem. Soc.* **2003**, *125*, 10997. (b) Kubo, T. doctoral thesis, Osaka University, 1996.
- (31) Yamanaka, S.; Okumura, M.; Nakano, M.; Yamaguchi, K. *J. Mol. Struct.* **1994**, *310*, 205.
- (32) Champagne, B.; Kirtman, B. In ref 8, Chapter 2, p 63.
- (33) Yamaguchi, K.; Tsunekawa, T.; Toyoda, Y.; Fueno, T. *Chem. Phys. Lett.* **1988**, *143*, 371.

- (34) Yamaguchi, K.; Okumura, M.; Maki, J.; Noro, T.; Namimoto, H.; Nakano, M.; Fueno, T.; Nakasuji, K. *Chem. Phys. Lett.* **1992**, *190*, 353.
- (35) Okumura, M.; Yamanaka, S.; Mori, W.; Yamaguchi, K. *J. Mol. Struct.* **1994**, *310*, 177.
- (36) Thouless, D. J. *The Quantum Mechanics of Many-Body Systems*; Academic Press: New York, 1961.
- (37) Ozaki, M.-A. *J. Math. Phys.* **1985**, *26*, 1521.
- (38) Bofill, J. M.; Pulay, P. *J. Chem. Phys.* **1989**, *90*, 3657.
- (39) Frisch, M. J.; Trucks, G. W.; Schlegel, H. B.; Scuseria, G. E.; Robb, M. A.; Cheeseman, J. R.; Zakrzewski, V. G.; Montgomery, J. A.; Stratmann, R. E.; Burant, J. C.; Dapprich, S.; Millam, J. M.; Daniels, A. D.; Kudin, K. N.; Strain, M. C.; Farkas, O.; Tomasi, J.; Barone, V.; Cossi, M.; Cammi, R.; Mennucci, B.; Pomelli, C.; Adamo, C.; Clifford, S.; Ochterski, J.; Petersson, G. A.; Ayala, P. Y.; Cui, Q.; Morokuma, K.; Malick, D. K.; Rabuck, A. D.; Raghavachari, K.; Foresman, J. B.; Cioslowski, J.; Ortiz, J. V.; Stefanov, B. B.; Liu, G.; Liashenko, A.; Piskorz, P.; Komaromi, I.; Gomperts, R.; Martin, R. L.; Fox, D. J.; Keith, T.; Al-Laham, M. A.; Peng, C. Y.; Nanayakkara, A.; Gonzalez, C.; Challacombe, M.; Gill, P. M. W.; Johnson, B. G.; Chen, W.; Wong, M. W.; Andres, J. L.; Head-Gordon, M.; Replogle, E. S.; Pople, J. A. *Gaussian 98*, revision A.1; Gaussian, Inc.: Pittsburgh, PA, 1998.
- (40) Cohen, H. D.; Roothaan, C. C. J. *J. Chem. Phys.* **1965**, *43*, S34.
- (41) Kitagawa, Y.; Soda, T.; Shigeta, Y.; Yamanaka, S.; Yoshioka, Y.; Yamaguchi, K. *Int. J. Quantum Chem.* **2001**, *84*, 592.
- (42) Kitagawa, Y.; Kawakami, T.; Yamaguchi, K. *Mol. Phys.* **2002**, *100*, 11, 1829.
- (43) (a) Krylov, A. I. *Chem. Phys. Lett.* **2001**, *338*, 375. (b) Krylov, A. I.; Sherrill C. D. *J. Chem. Phys.* **2002**, *116*, 3194.